Biomechanics of Joints and Orthopaedic Implants
Professor Sanjay Gupta
Department of Mechanical Engineering
Indian Institute of Technology, Kharagpur
Lecture 33
Experimental Validation of Pre-Clinical Analysis

Good morning everybody. Welcome to the fifth lecture of module 6 on Experimental Validation of Preclinical Analysis.

(Refer Slide Time: 00:42)

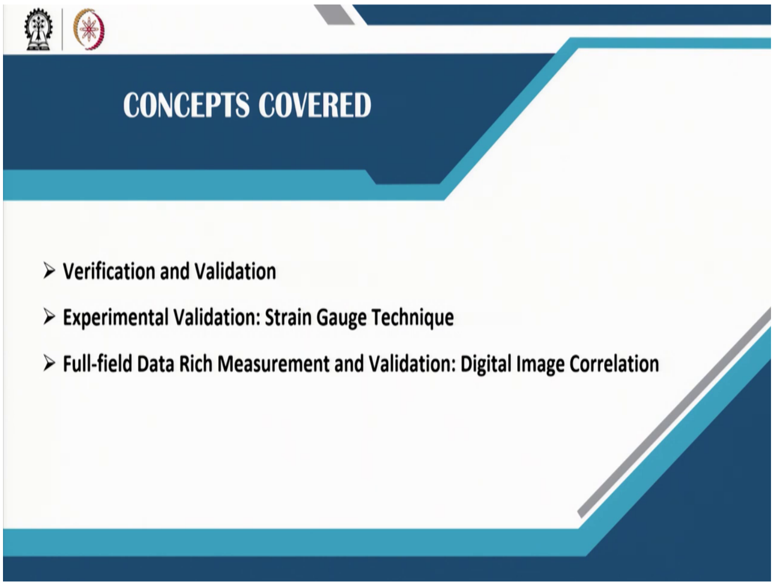

In this lecture, we will be discussing about the aspects of validation and verification. Then we will discuss experimental validation using strain gauge technique, and finally, we will discuss about a full field data rich measurement used for validation that is the digital image correlation technique.

(Refer Slide Time: 01:10)

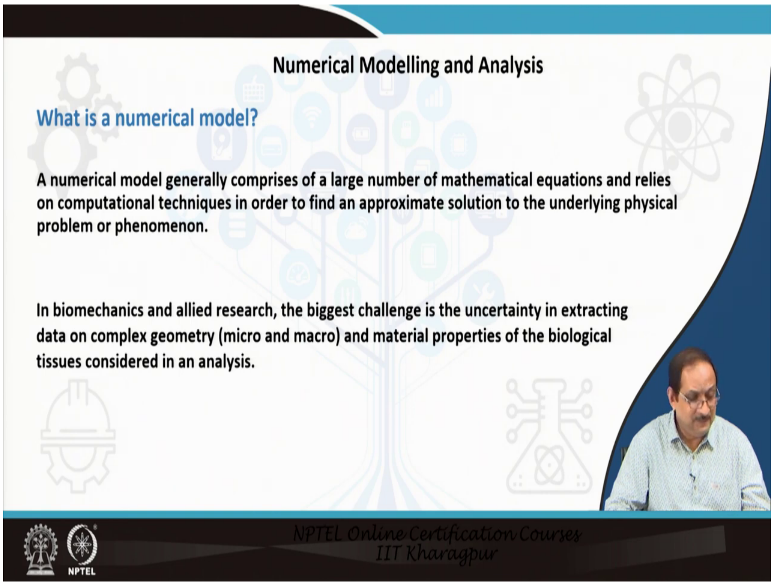

Now, before I move to the details of the experimental validation, let us first define what is a numerical model? Now, a numerical model generally comprises of a large number of mathematical equations and relies on computational techniques in order to find an approximate solution to the underlying physical problem or phenomenon.

Now, owing to their ability to represent complex systems, numerical models are used to simulate and study a large variety of problems in biomechanics, ranging from structural analysis and mass transport to fluid mechanics.

In biomechanics and allied research, the biggest challenge is the uncertainty in extracting data on complex geometry, both for micro and macro models and material properties of the biological tissues considered in an analysis. The tools and techniques such as finite element modelling and analysis are valid only when they are used correctly.

(Refer Slide Time: 02:47)

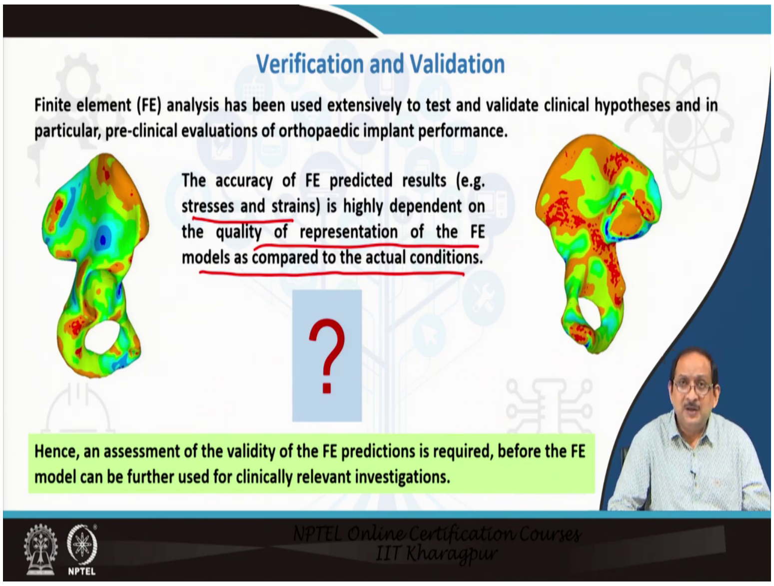

Finite element analysis has been extensively used to test and validate clinical hypotheses and in particular pre-clinical evaluations of orthopaedic implant performance.

The accuracy of the predicted results from this finite element analysis, Say, for instance, we are predicting stresses and strain distribution, which is highly dependent on the quality of representation of the FE models as compared to the actual conditions. Hence, an assessment of the validity of the FE predictions is required before the FE model can be further used for clinically relevant investigations.

(Refer Slide Time: 03:54)

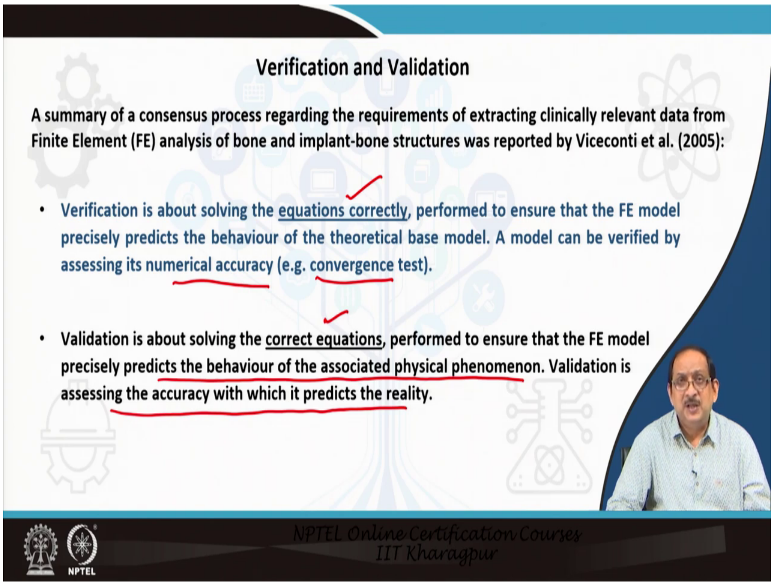

Now, let us talk about verification and validation. Now a summary of a consensus process regarding the requirements of extracting clinically relevant data from finite element analysis of bone and implant-bone structures was reported by Viceconti. This has been discussed in this editorial paper and it contains certain guidelines that need to be performed for verification and validation of the pre-clinical analysis or evaluations that we often use for biomechanical evaluation.

Verification is about solving the equations correctly. Now, it is performed to ensure that the FE model precisely predicts the behaviour of the theoretical model. A model can be verified by assessing its numerical accuracy, for example, using a convergence test. So, verification is about solving the equations correctly and we can employ the convergence test in order to verify the results of a finite element model; how sensitive is the model to changes in element sizes for example.

Validation is about solving the correct equations performed to ensure that the FE model precisely predicts the behaviour of the associated physical phenomenon. Therefore, validation is assessing the accuracy with which it predicts the reality.

(Refer Slide Time: 06:26)

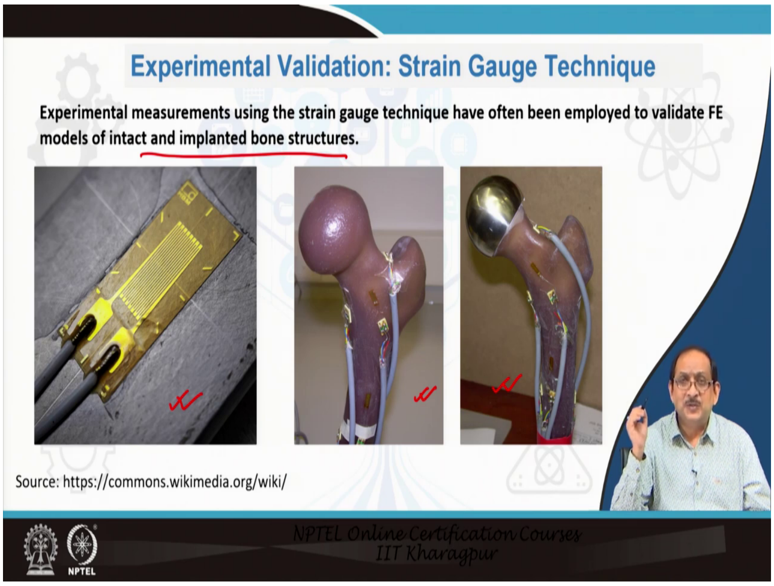

Now, let us move into the second topic, which is on experimental validation using the age-old strain gauge technique. Now, experimental measurements using the strain gauge technique have often been employed to validate FE models of intact and implanted bone structures. So, as you can see, in this slide on the left, we have a typical strain gauge that is generally glued on the surface of maybe an intact model or an implanted model as shown in the figure, and then we can actually measure the strains due to some applied load.

(Refer Slide Time: 07:26)

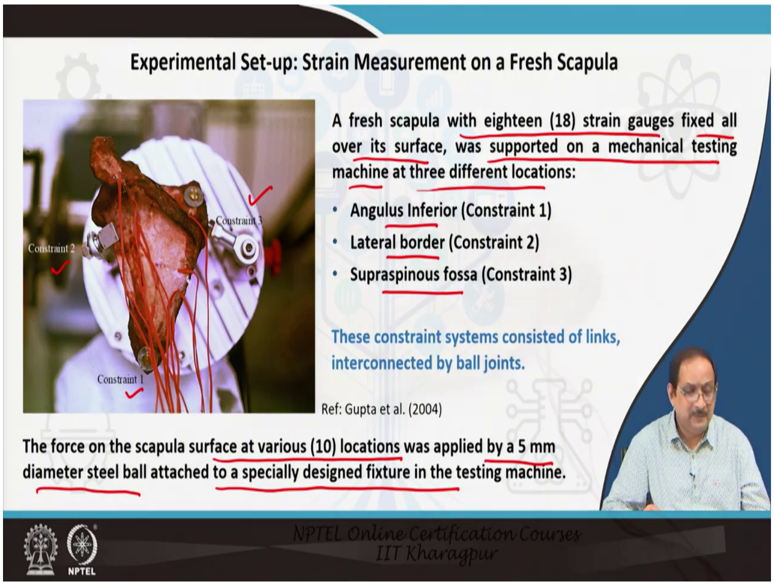

Now, I would like to discuss about strain measurement on a fresh sample of bone and that sample of bone is a scapula. So, it is a fresh sample of bone taken out from donated cadavers and this had been used for experimental validation of a finite element model. Now, fresh scapula with 18 strain gauges is fixed all over its surface.

So, the strain gauges were fixed and distributed randomly all over the surface and the fresh scapula with the 18 strain gauges was supported on a mechanical testing machine at three different locations, as you can see at the angulus inferior, which is constraint one. At the lateral border is constraint two, which is clearly seen in the figure presented in the slide and another constraint is at the supraspinous fossa, which is constrained three as indicated in the figure.

Now, these constraint systems consist of links interconnected by ball joints. We will discuss about this in the next slide. But these constraint systems are used to support the fresh scapula on which 18 strain gauges are fixed all over the surface.

So, we had applied the forces at ten different locations and this force was applied by a 5 mm diameter steel ball attached to a specially designed fixture in the mechanical testing machine.

(Refer Slide Time: 09:55)

Let me present to you a plastic model of a scapula, a plastic model of scapular on which you can see two strain gauges fixed on the surface of the scapula. This plastic model was used as a pilot study before the measurements on a fresh sample of scapula were undertaken. Here you can see two holes, one on the angulus inferior and the other in the fossa area, through which the supporting link mechanisms are attached.

(Refer Slide Time: 10:38)

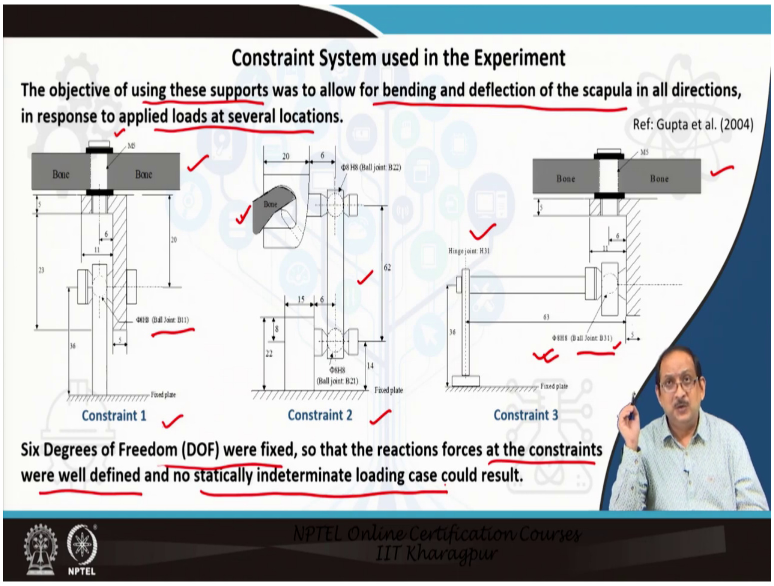

Let us discuss briefly about the constraint system used in the experiment. The objective of using these supports or constraint systems was to allow bending and deflection of the scapula in all directions in response to applied loads at several locations. So, constraint number one as you can see, a detailed diagram of constraint one is presented here.

It has this ball joint and you can see the bone is held by a bolted joint here. A hole is drilled within the bone through which a bolt is fixed to the supporting links. Constraint number two is presented here, as you can see, so it also has a similar type of supporting arrangements with ball joints, and the bone is held by a jaw which is further fixed to the supporting links as shown here.

Constraint number three again has a drilled hole within the bone. So, a bolt is connected to the supporting links, which have a ball joint and a hinge joint. Now, the 6 degrees of freedom of this support system were fixed so that the reaction forces at the constraints were well defined, and no statically indeterminate loading case could result.

(Refer Slide Time: 12:47)

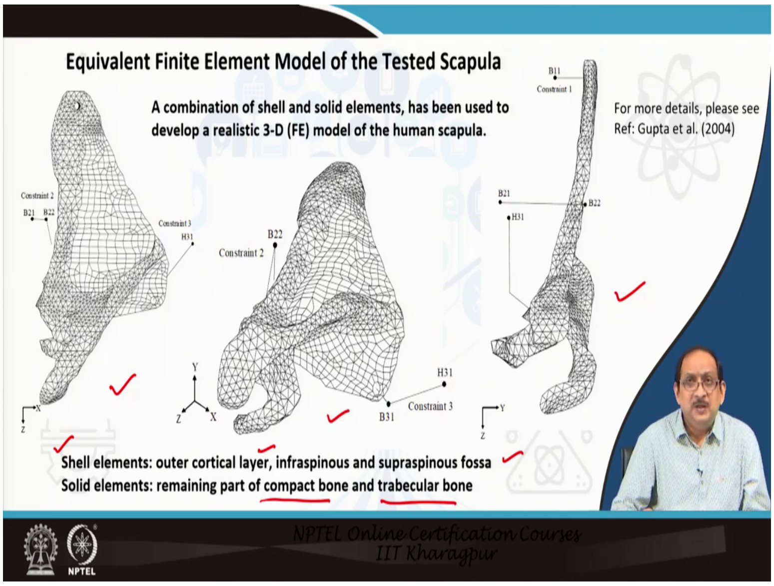

So, after the experiment was carried out, we actually developed an equivalent finite element model of the tested scapula. So, in this slide, you can see in three views the finite element model of the tested scapula. A novel approach, a combination of shell and solid elements, was used in the study, which was particularly appropriate to develop a realistic 3D finite element model of the human scapula.

The scapula, as you already know, consists of thin flat bony regions and some solid bony ridges. So, the shell elements were used to model the outer cortical layer, infraspinatus fossa and supraspinous fossa, which are flat laminated type of bony structures and the solid elements were used to model the remaining part of the compact bone and the trabecular bone in the solid bony ridges of the scapula.

(Refer Slide Time: 14:20)

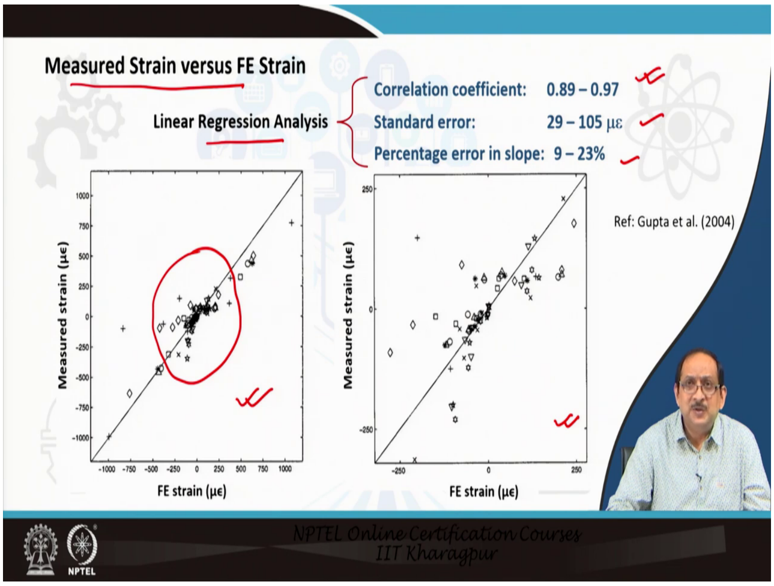

Now, let us compare measured strain and finite element strain as indicated in the figure. So, the figure on the left, as you can see here, consists of all the measured data, but the figure on the right is plotting a zoomed view or closer view of a cluster of data in the range of ± 250 micro strain. So, that is in the low range of ± 250 micro strain.

Now, when we perform a linear regression analysis between the two bivariant data or independent data, measured strain and finite element strain, we actually find a correlation coefficient varying between points 0.89 to 0.97. A standard error varying between 29 to 105 microstrain and a percentage error in slope that was found out was 9 to 23 percent.

Based on the results of the linear regression analysis, we can conclude that the finite element model can be further used for pre-clinical evaluations or analysis since it predicts realistic estimates of stresses and strains.

(Refer Slide Time: 16:31)

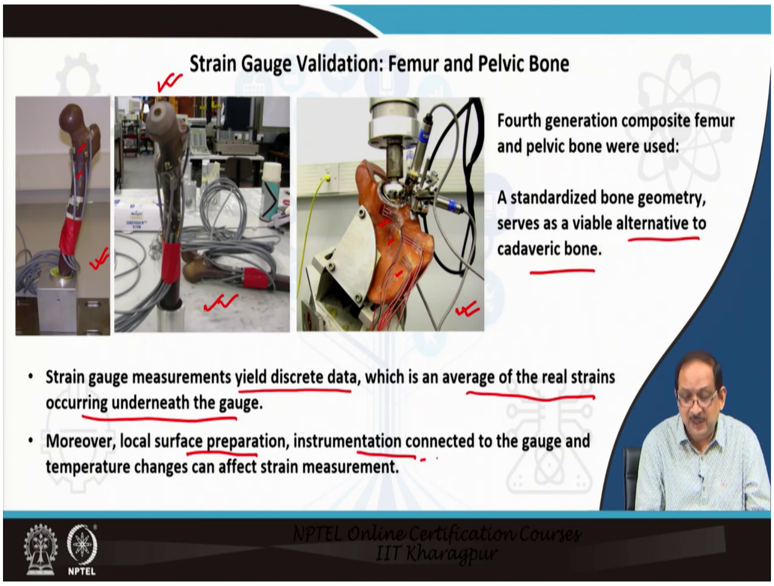

Now, we will be discussing about strain gauge validation on the femur and pelvic bone, both intact and implanted bone structures. Now, with time fourth-generation composite bones have evolved, and they have been commonly used in experimental investigations of biomechanical structures like implant and implant-bone structures.

Now, these composite bones have a standardized bone geometry, and they serve as a viable alternative to the cadaveric bone that has been earlier used for testing. Now, here in this slide, you can see a photo of the intact composite femur, and on the right, you can see a photo of the test setup of a pelvic bone with linear displacement sensors and, of course, the strain gauges and rosettes that are fixed on the surface of the bone.

So, in both the femur bone and the pelvic bone, the strain gauges are visible and the connecting wires from the strain gauges goes to a strain amplifier. Now, here we can see that a composite femur bone has been machined to fit and resurfacing implant, which will be later tested using the strain gauge technique.

Now, strain gauge measurements, as you might know, yield discrete data which is an average of the real strains occurring underneath the gauge. Moreover, local surface preparation, instrumentation connected to the gauge and temperature changes can actually affect strain measurement.

(Refer Slide Time: 19:14)

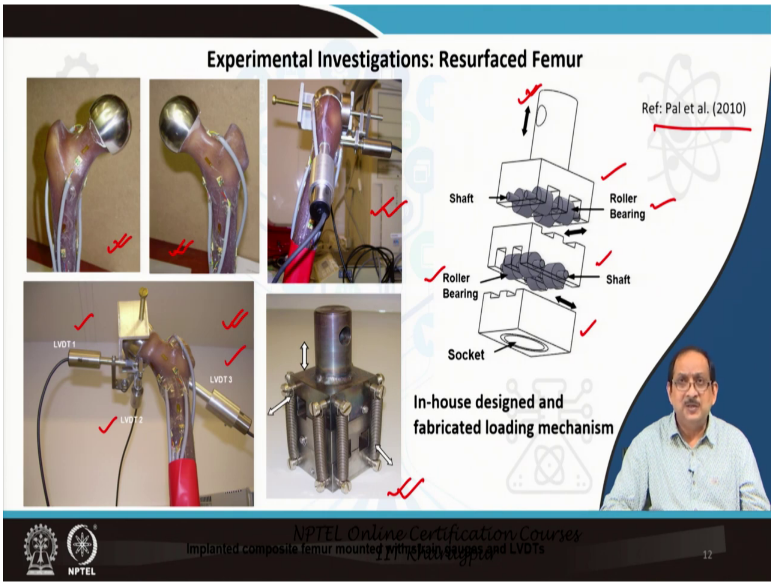

In this slide, we will be focusing on the resurfaced femur. So, as you can see in the figure, on the left, the two figures facing opposite to each other are photos from the experiment, and here you can see the strain gauges are fixed at different locations on the implanted femur. Now, apart from the strain gauges, there were LVDTs, linear displacement sensors to measure displacements or relative displacement between bone and implant.

So, three LVDTs were fixed to measure implant-bone relative displacements in different directions. So, two views are presented here; the figure, as I have marked here at the bottom of the slide, is an in-house designed and fabricated loading mechanism. Now, let us look into the details of this loading mechanism, which is used to apply the vertical load from the top on the femur head or on the implant in the mechanical testing machine.

The loading fixture actually consisted of three blocks, as you can see here, in the slide with two sets of crosswise roller bearings. So the roller bearings are two sets of roller bearings, but they are in two different directions and are in perpendicular directions so that the blocks can actually move relatively in two principal directions when it is actually compressed from the top.

So, these crosswise roller bearings are arranged in between these three blocks. The roller bearings were oriented along two perpendicular directions in order to allow movements between the blocks in the transverse plane and to accommodate deformation of the femur due to the application of a vertical compressive force. More details can be found in our publication in the journal of biomechanics in 2010.

(Refer Slide Time: 22:36)

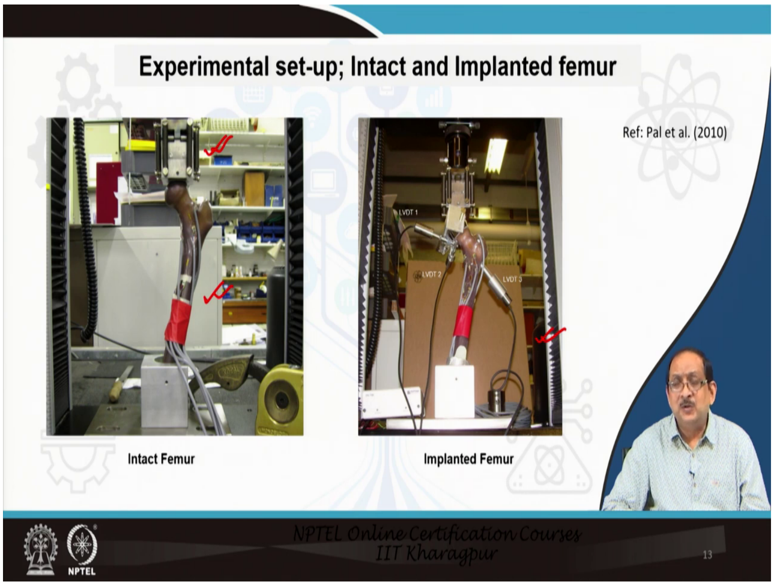

So, let us now see the experimental setup where we tested. You can see the loading fixture and the intact femur is fixed or positioned, maintaining the anatomical angles and it is held in a mechanical testing machine. On the right, we have the implanted femur and this is also held in a similar way with the load application mechanism on the top.

(Refer Slide Time: 23:23)

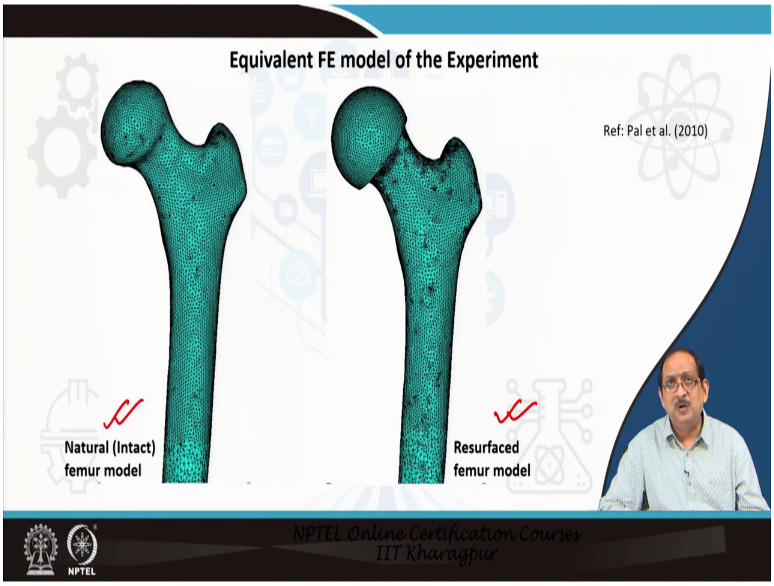

Now, after performing the experiment, we have developed the finite element models of the intact femur and the resurfaced femur. This is actually an equivalent finite element model of the experiment.

(Refer Slide Time: 23:47)

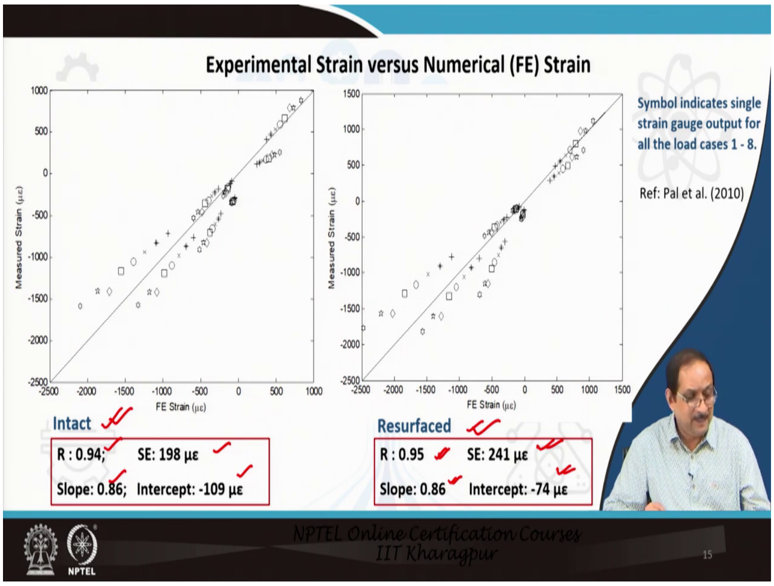

Let us come to the results. The results are actually presented in the form of comparison between experimental strain and numerical or FE predicted strain. So, on the left, we have the results corresponding to the intact femur, and on the right, we have the results corresponding to the resurfaced femur. In the figure, one symbol indicates single strain gauge output for all the load cases from 1 to 8. There are eight load cases. So, each symbol corresponds to a single strain gauge output.

Now, when we perform the regression analysis, we see the correlation coefficient of 0.94 and standard error of 198 microstrain. The slope is pretty much close to 1 and the intercept is -109 microstrain, which is actually small compared to the range of strains that have been measured. So, for the intact femur, there is a very close linear relationship between the FE predicted strain and the measured strain.

Now, if we consider the resurfaced femur, we see a slightly higher correlation coefficient. The slope is about the same 0.86, but the intercept is closer to 0. So, the slope is close to 1, the intercept is close to 0, -74 microstrain and the standard error of the estimate was 241 microstrain. So, from this linear regression analysis, we can conclude that for both intact and resurfaced femur, the measured strain has a close linear relationship with the FE predicted strains.

(Refer Slide Time: 26:26)

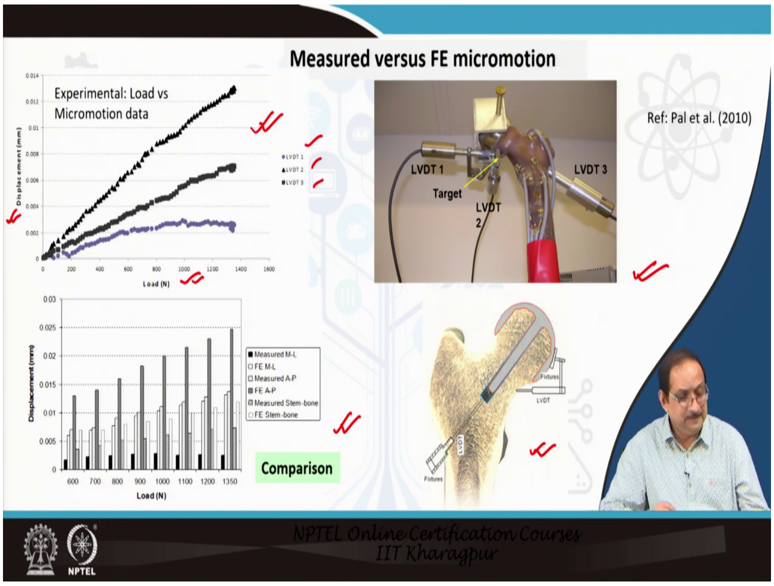

Let us now present the results of measured micromotion versus the FE predicted micromotion. On the left, you can see the experimental data. So, we have the load on the x-axis and the micromotion or displacement recorded by the three LVDTs 1, 2, and 3 presented here in the graph.

Now, when we compare the results predicted by the FE model and the measured micromotion, we see that the trends are similar, although there are some quantitative deviations between the two variables, which is the measured micromotion and the FE predicted micromotion. The figure presented on the right is the LVDTs, and you can see a more detailed view of the LVDTs is presented in a sketch in the slide.

(Refer Slide Time: 28:05)

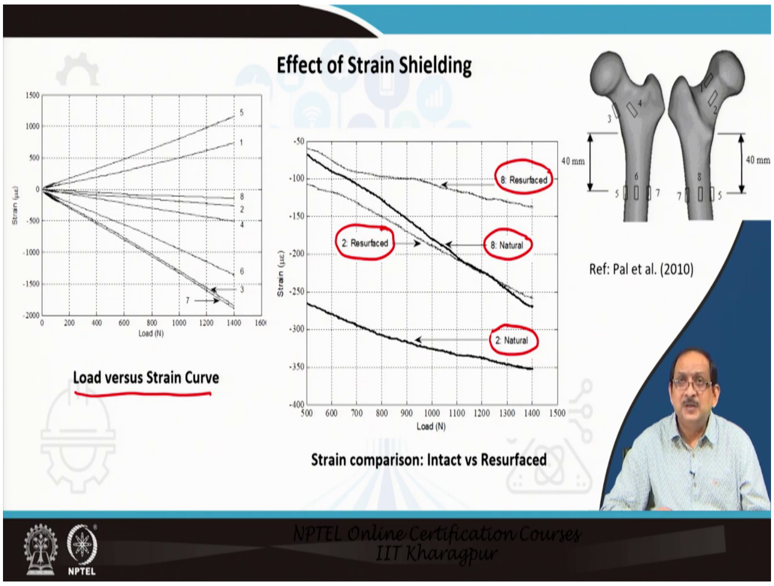

The effect of strain shielding is evident from the experimental measurements, as you can see here in the slide. So, the load versus strain curve is plotted for eight strain gauges, as you can see here. Now, we will focus our attention on strain gauge 2, so it is located exactly at similar positions.

So, strain gauge 2 in natural and strain gauge 2 in the implanted femur can be compared. Similarly, strain gauge 8 in natural and strain gauge 8 in resurfaced or implanted measurements can be compared. So, it is clearly evident that after implantation, the strain recorded in the implanted femur or resurfaced femur is considerably less as compared to the natural situation.

(Refer Slide Time: 29:33)

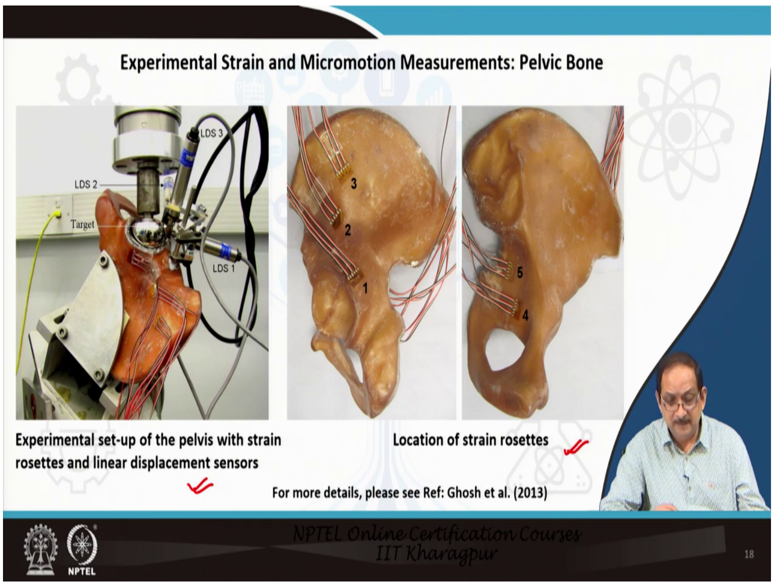

Now, let us discuss about the experimental strain and micromotion measurements on a pelvic bone. On the left, you can see the experimental setup of the pelvis with strain rosettes and linear displacement sensors. So, the linear displacement sensors are oriented along mutually orthogonal directions. So, LDS 1, 2, and 3 are oriented along three perpendicular directions. On the right, we have the location of strain rosettes fixed on the surface of the composite pelvis or composite pelvic bone.

(Refer Slide Time: 30:25)

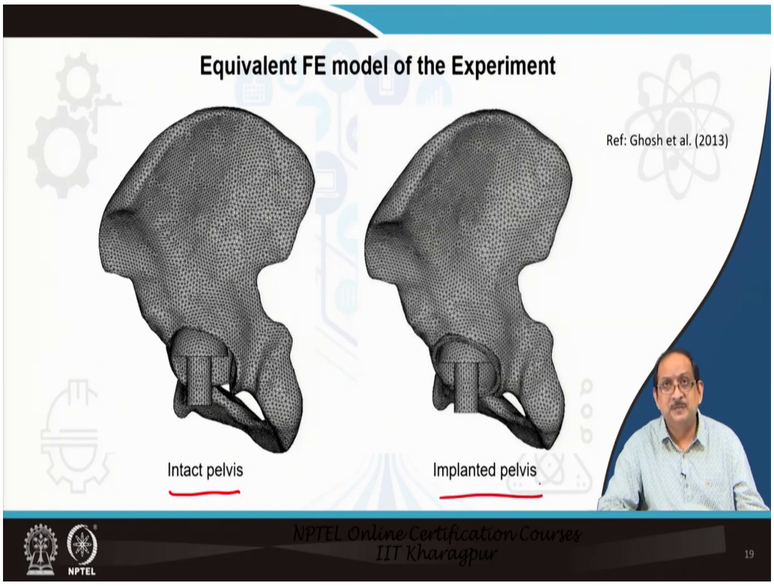

The equivalent FE model of the experiment was developed, as you can see here and now presented in this slide for the intact pelvis and the implanted pelvis.

(Refer Slide Time: 30:42)

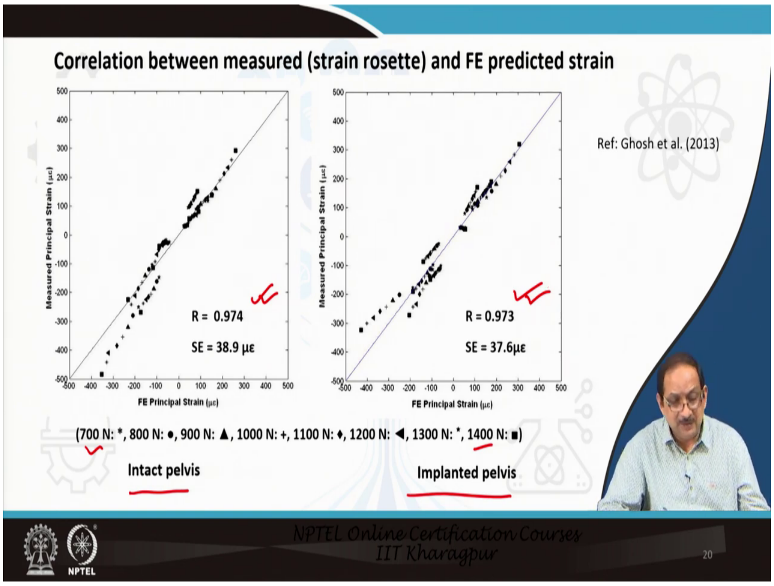

Let us come to the results that is the correlation between the measured strain and the FE predicted strain. So, here we have several load cases as indicated from 700 to 1400 in steps of 100 Newtons. We have increased the load and we have recorded the measurement as well as we have calculated the FE strains at comparable locations.

So, when we compare the FE predicted principal strains with the measured principal strains by the strain rosettes, we see that the measured strains are very well comparable to the FE predicted strain as indicated by the linear regression analysis as presented in the slide.

(Refer Slide Time: 31:41)

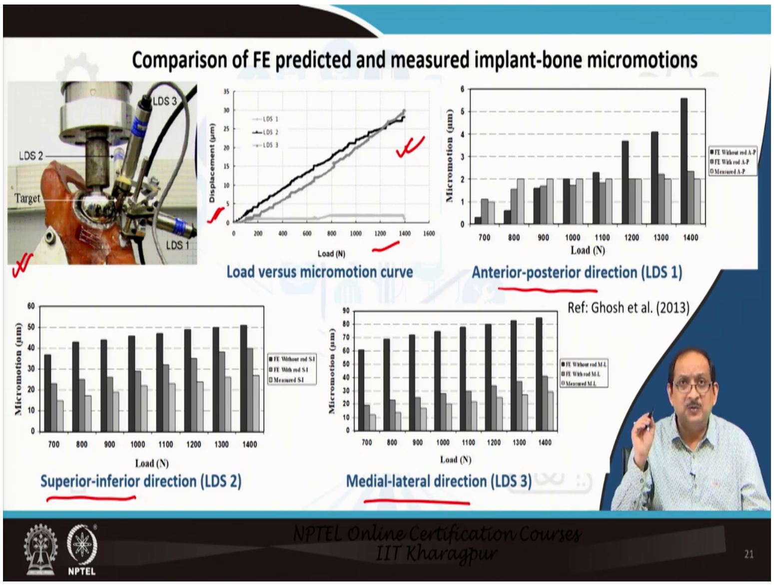

Let us now compare the FE predicted and measured implant-bone micromotion. So, we have measured the micromotions or displacements against load, and the load versus the micromotion curve is presented here in the slide, based on the experiment performed here.

Now, we compare the measurements with the FE predicted data along three directions, which are the anterior-posterior direction, superior-inferior direction, and medial-lateral direction. Corresponding to LDS 1, 2, and 3, we clearly observed that the trends are comparable. Although there are some quantitative deviations between the measured micromotion and the FE predicted micromotion.

(Refer Slide Time: 32:47)

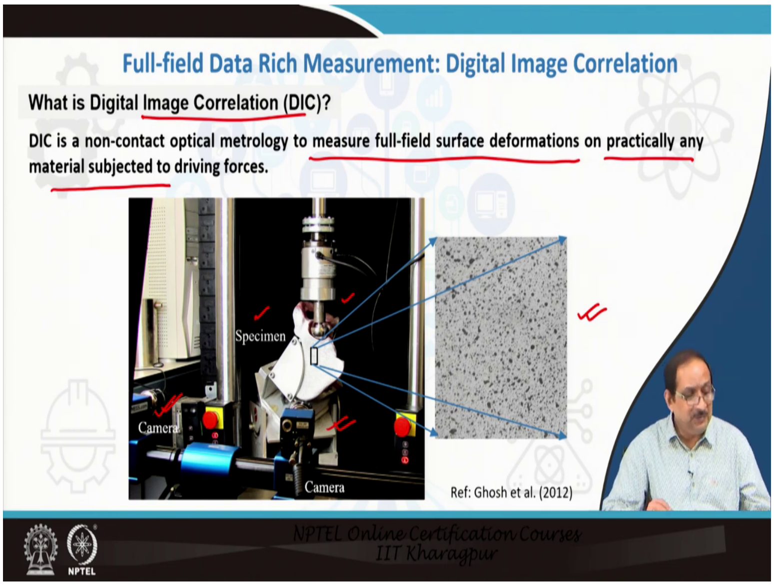

We will now move into the third topic, which is quite interesting. This is regarding the full field data rich measurement using the digital image correlation technique. Now, what is digital image correlation? DIC is a non-contact optical measurement technique to measure full-field surface deformations on practically any material subjected to driving forces or subjected to loadings.

So, here in the slide, you can see a photo of an experiment conducted by us on a pelvic bone. Now, apart from the digital correlation technique, in recent times, there has been another novel technique known as digital volume correlation, which has evolved for full-field 3D strain and deformation measurements. The technique imports volume image of the component in reference and deformed states and is able to calculate the full 3D displacement and strain map.

So, the digital volume correlation is a powerful and non-intrusive technique for the identification of subsurface material deformation and is capable of identifying defects, discontinuities, or other material characteristics.

Now, let us come back to the discussion on the digital image correlation technique. So, in this technique, you can see that we have the pelvic bone specimen loaded on the machine and the pelvic bone specimen has white paint on it. So, on top of the white paint, we need to spray or generate black speckle patterns, and the displacements of the speckle patterns need to be recorded by two cameras. So, DIC is a non-contact optical measurement technique to measure the full-field surface deformations in a selected region of interest.

(Refer Slide Time: 35:51)

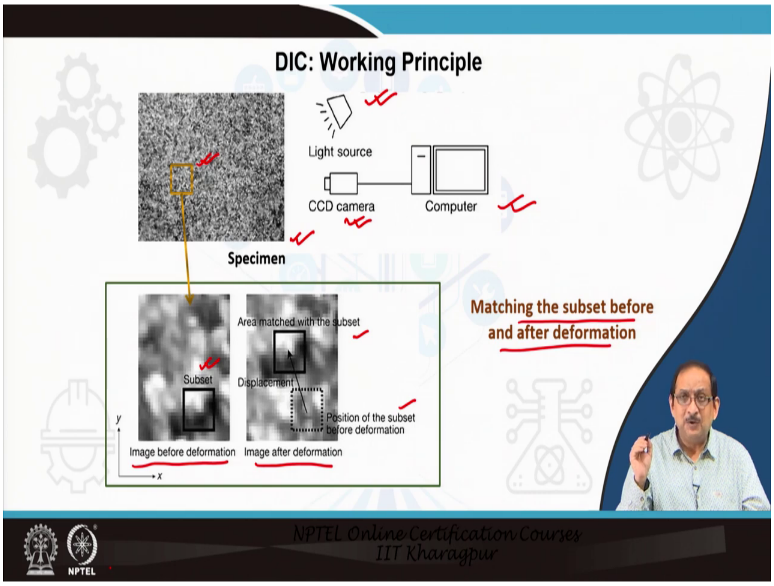

Let us briefly discuss about the working principle of the digital image correlation technique. So, as indicated earlier, you can see that there is a white light source, the digital cameras to record the deformation of the speckle pattern and the digital cameras are connected to the console or the computer.

So, the specimen having the black speckle pattern on white paint, the images of these specimens are acquired by the digital camera. So, the region of interest is located, and we are interested in the image before deformation and the image after deformation. So, a subset is constructed and the movement of this subset from the position before deformation to the position after deformation is recorded. Matching the subset before and after deformation is required to be executed by the DIC technique based on which we can calculate stains.

(Refer Slide Time: 37:28)

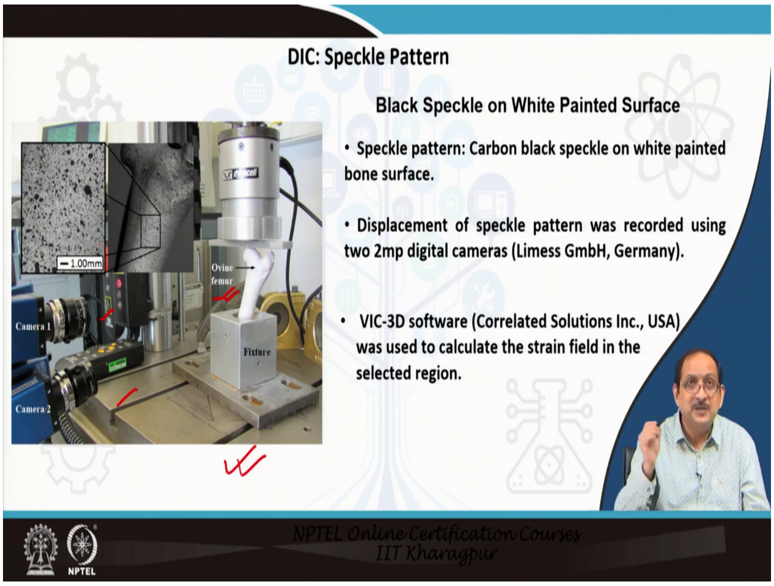

Now, let us discuss a little bit more in detail about the speckle pattern because the speckle pattern influences the DIC results. So, we had applied black speckle on white painted surface. So, the displacement of the speckle pattern was recorded using 2-megapixel digital cameras and with 3D software, which was used to calculate the strain field in the selected region. On the left, a typical setup of the DIC is shown with an ovine femur sample being tested using the two cameras, and of course, the speckle pattern is shown in the exploded view.

(Refer Slide Time: 38:33)

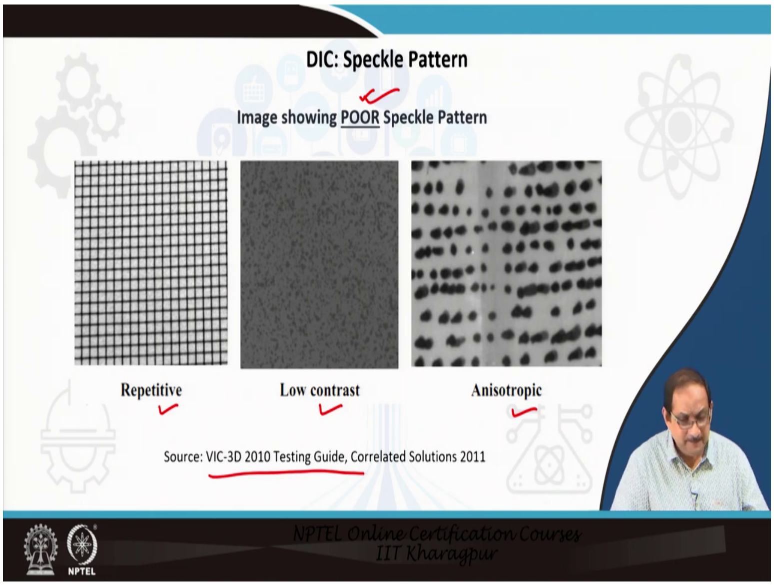

The quality of the generative speckle pattern has an important influence on the results of the DIC technique. Now, in this slide, the image shown here are examples of poor speckle pattern. The speckle patterns which are repetitive, low contrast and anisotropic in nature are considered to be poor speckle pattern and is expected to give doubtful results as specified by the VIC-3D testing guide.

(Refer Slide Time: 39:21)

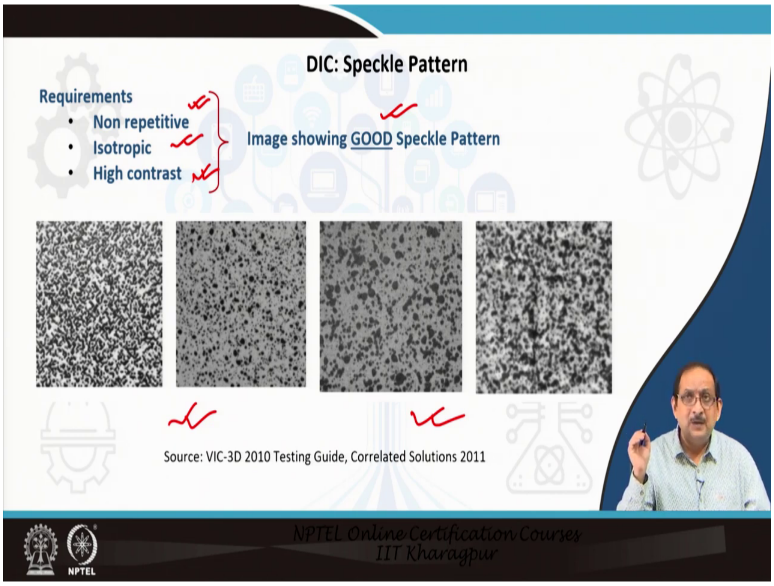

Now, in this slide, images of some good speckle pattern are presented. As you can see, the requirements are a non-repetitive type of randomized speckle pattern. The speckle pattern should be isotropic and have high contrast, as indicated in the four images. So, this sort of good speckle pattern is expected to give desired results using the DIC technique.

(Refer Slide Time: 40:00)

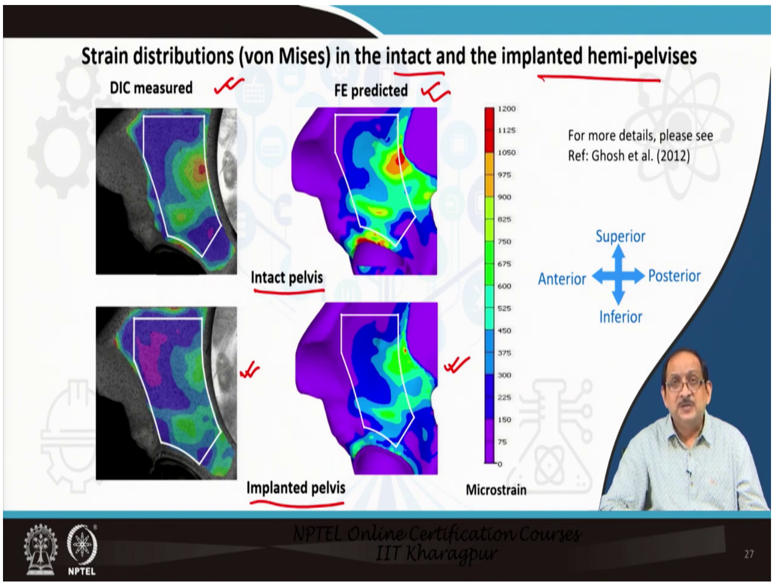

Now, we present the results of our study. So the von Mises strain distribution in intact and implanted Hemi pelvises, as you can see for the intact case, the area enclosed by the white line in the region of interest and you can see very clearly that the full-field strain distribution for the DIC measured case and the FE predicted case are very well comparable. Similar observations can be made for the implanted pelvis, wherein the DIC measured strains are very well comparable to the FE predicted strains.

(Refer Slide Time: 40:53)

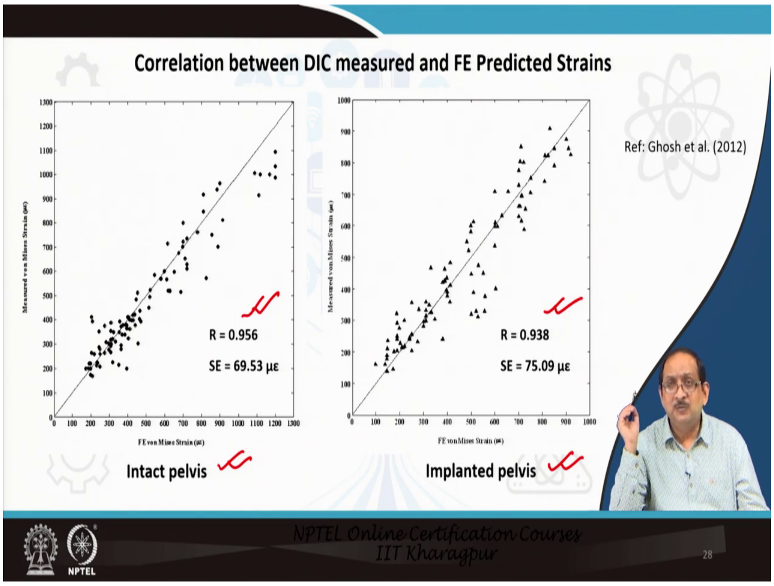

Now, we compare quantitative values of DIC measured strains and FE predicted strains. For the intact pelvis and the implanted pelvis, we can compare the DIC measured and FE predicted strain and you can clearly see the high correlation between the measured strain and the FE predicted strain for both cases.

(Refer Slide Time: 41:22)

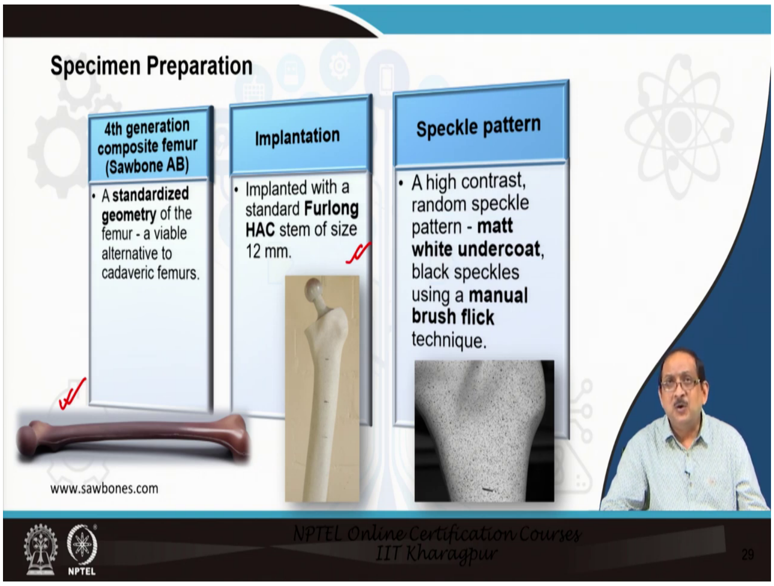

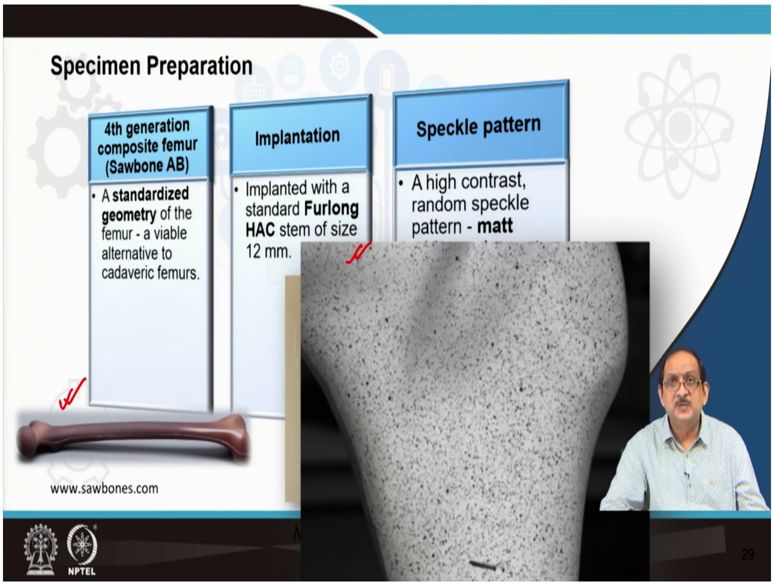

Next, we will be discussing about testing the femur with a total joint replacement femoral component. Now, quickly we will go through the specimen preparations; as you can see, we use the fourth-generation composite femur from sawbones. We actually do the implantation by taking help from an orthopaedic surgeon and following the standard surgical procedure.

So, implant with the standard Furlong HAC stem of size 12 millimeter has been implanted within this composite bone, and we actually generate the high contrast random speckle pattern, with a matt white undercoat, black speckles using a manual brush flick technique. So, we are using a toothbrush and we flick the paint on a white undercoat paint which has a matt finish.

(Refer Slide Time: 42:56)

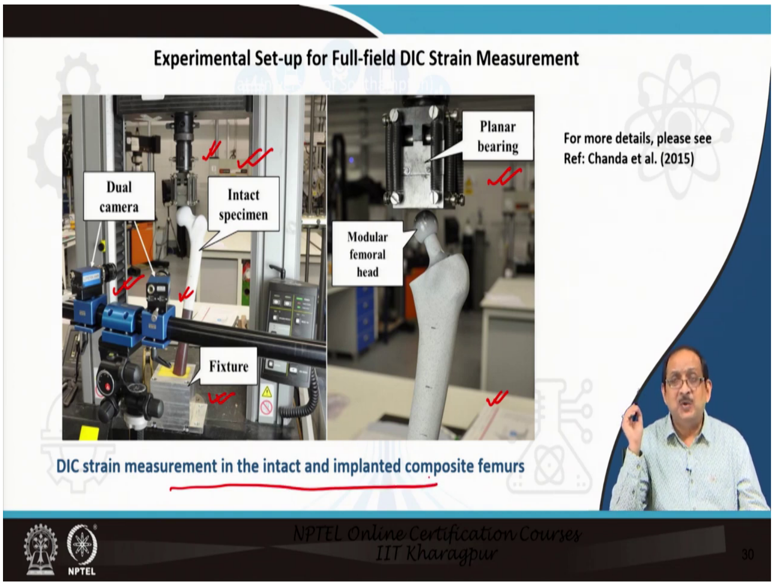

The experimental setup for the full field DIC measurement is presented here. On the left, we have the intact specimen, we have the dual cameras, and of course, the fixture on which the bone is fixed and the loading mechanism that we have used earlier is used here to apply the vertical load.

On the right, we have the implanted femur with the load application mechanism containing the planer bearings. So, this is the DIC strain measurement setup for the intact and implanted composite femurs.

(Refer Slide Time: 43:46)

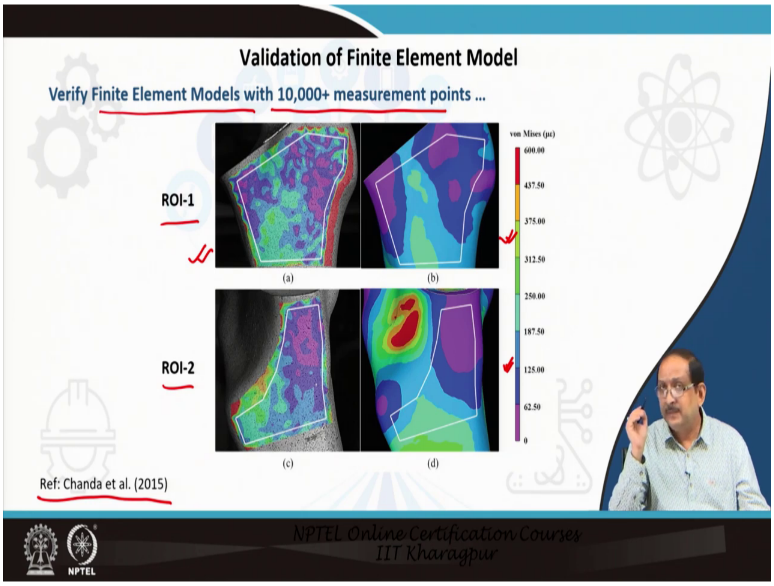

Let me now present the results. So, we have verified basically the finite element models with more than 10,000 measurement points. So, we are presenting results for the region of interest

1 and region of interest 2 as observed, as can be seen in this slide. So, in both the region of interest, you can see here very clearly that the DIC measured strain is very well comparable to the FE predicted strains.

(Refer Slide Time: 44:47)

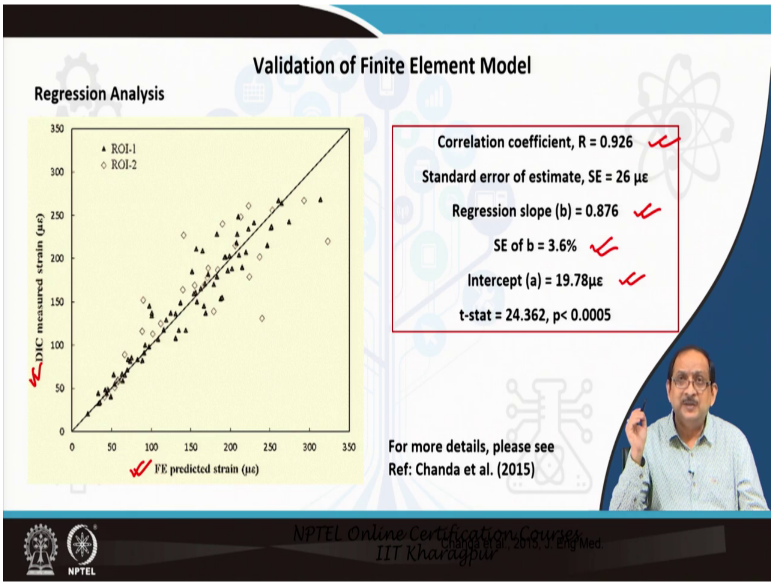

So, if we perform a regression analysis of the data, the DIC measured data and FE predicted data, we find the correlation coefficient R is equal to 0.926, standard error of 26 microstrain the regression slope is about 0.876, which is close to 1 and we have this low standard error of the regression slope 3.6 percent. The intercept is also close to 0, 19.78 microstrain. So, we may conclude that the DIC measured strain is very closely related to the FE predicted strain and it is related by a linear relationship.

(Refer Slide Time: 45:53)

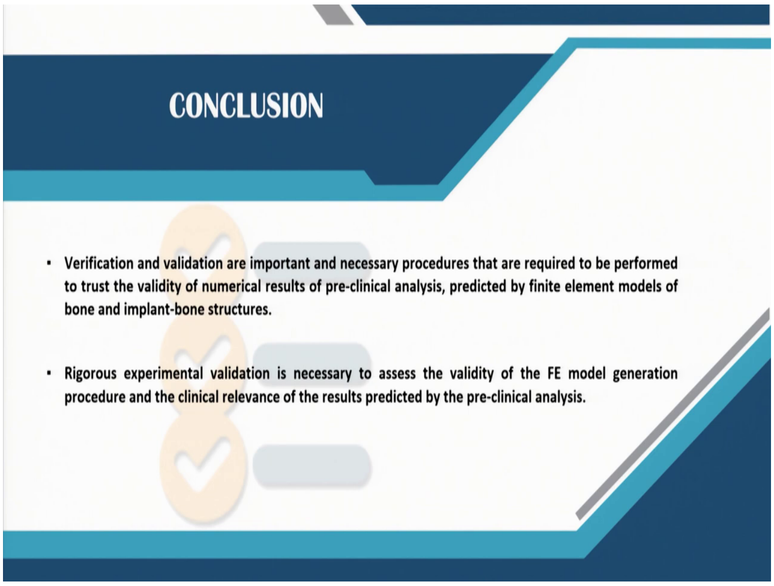

Let us come to the conclusions of this lecture. Verification and validation are important and necessary procedures that are required to be performed to trust the validity of numerical results of pre-clinical analysis, predicted by finite element models of bone and implant-bone structures. Rigorous experimental validation is necessary to assess the validity of the FE model generation procedure and the clinical relevance of the results predicted by the pre-clinical analysis.

(Refer Slide Time: 46:37)

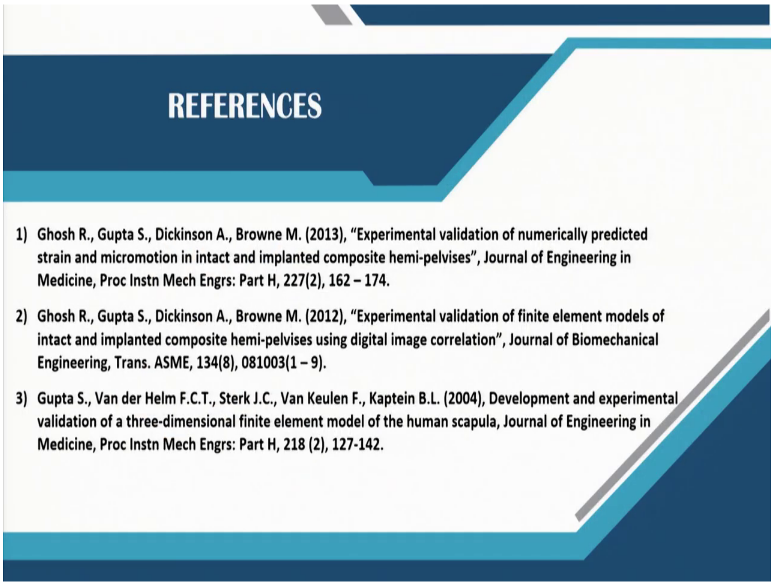

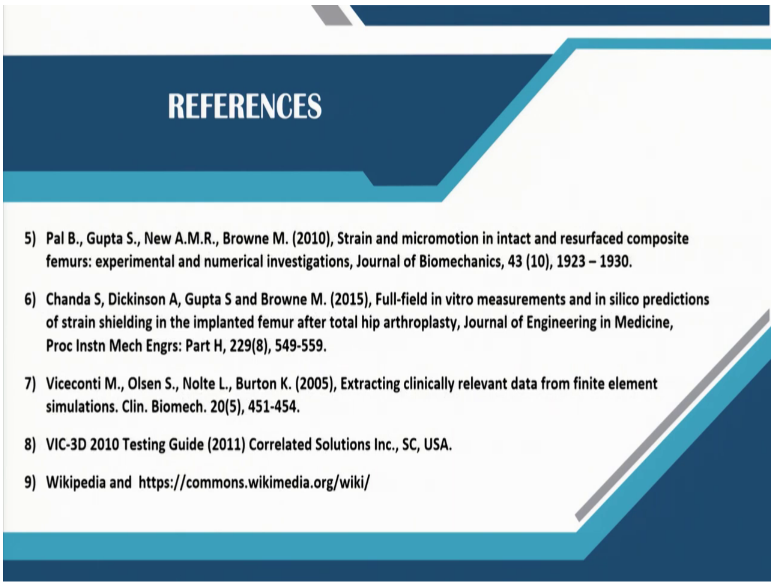

The list of references is presented in two slides based on which the lecture has been prepared. Thank you for listening.